Proceedings of the 1998 IEEE
International Conference on Robotics & Automation
Leuven, Belgium • May 1998

Task-Priority Redundancy Resolution for Underwater Vehicle-Manipulator Systems

Gianluca Antonelli Stefano Chiaverini

Dipartimento di Informatica e Sistemistica
Università degli Studi di Napoli "Federico II"
via Claudio 21, 80125 Napoli, Italy

Abstract

An underwater vehicle-manipulator system (UVMS) usually has more degrees of freedom than those required to attain given end-effector postures. Therefore, the UVMS is a redundant system and kinematic control algorithms can be applied aimed at achieving additional control objectives such as energy savings or increase of system manipulability. This paper presents a task-priority inverse kinematics approach to redundancy resolution for a UVMS. Three case studies are developed to demonstrate effectiveness of the technique in different applications.

1. Introduction

A system is kinematically redundant when it possesses more degrees of freedom than those required to execute a given task. Since a general manipulation task is specified in terms of given position and orientation trajectories to the end-effector of a robot arm, strictly speaking an underwater vehicle-manipulator system (UVMS) is always kinematically redundant due to the degrees of freedom provided by the vehicle itself. On the other hand, it is not always efficient to use vehicle thrusters to move the manipulator end effector because of the vehicle inertia which is usually bigger than the inertia of the sole manipulator arm.

If the manipulation task must be executed in a confined space (e.g., underwater structure maintenance), the vehicle is used to ensure station keeping, i.e. to counteract environmental disturbances, restoring forces, and the dynamic interactions between the vehicle and the manipulator [10]. When execution of the task requires large displacements (e.g., pipeline inspection), the vehicle is used to provide wide and slow motion of the manipulator base while the manipulator provides fast and accurate motion of the end-effector [4]. In a sense, the vehicle gives an unlimited operational space to the manipulator.

According to the above, a redundancy resolution technique might be useful to achieve system coordination in such a way as to guarantee end-effector tracking accuracy and, at the same time, additional control objectives, e.g. energy savings or increase of system manipulability. To this purpose the task-priority redundancy resolution technique [7,8] is well suited in that it allows the specification of a primary task which is fulfilled with higher priority with respect to a secondary task. In the case of a UVMS, the typical primary task might be a given end-effector posture while examples of secondary tasks include reduction of fuel consumption, improvement of system manipulability, and obstacle avoidance.

The goal of this paper is to develop a task-priority redundancy resolution technique for kinematic control of UVMS. The proposed approach is based on the work in [2] and thus is robust to the occurrence of algorithmic singularities. Simulations have been developed on a UVMS constituted by the NPS AUV II [6] carrying a three-link planar manipulator. A first case study is aimed at accomplishing reduction of energy consumption associated to compensation of the environmental disturbances while tracking a given end-effector trajectory. This can be obtained for vehicles of suitable shape by requiring alignment of the vehicle fore aft direction with the ocean current; of course, this would not be applicable to spherical-body vehicles, e.g. the one described in [3]. A second case study is aimed at maintaining high dexterity of the manipulator arm while tracking a given end-effector trajectory with minimal vehicle motion. A third case study develops a performance comparison in terms of energy consumption of the control law described in the first case study with respect to a fixed vehicle orientation control law in a station keeping task. The obtained results show the effectiveness of the proposed techniques.

2. Dynamic modelling

Effective control of the UVMS requires accurate knowledge of its dynamics in order to apply model-based dynamic compensation. The equation of motions of the UVMS in a body-fixed reference frame can be written in the form [9]

$$\boldsymbol{M}(\boldsymbol{q})\dot{\boldsymbol{\zeta}} + \boldsymbol{C}(\boldsymbol{q},\boldsymbol{\zeta})\boldsymbol{\zeta} + \boldsymbol{D}(\boldsymbol{q},\boldsymbol{\zeta})\boldsymbol{\zeta} + \boldsymbol{g}(\boldsymbol{q},\boldsymbol{\eta}) = \boldsymbol{\tau}, \quad (1)$$

where $\boldsymbol{\zeta} = [\boldsymbol{\nu}^T, \dot{\boldsymbol{q}}^T]^T$, $\boldsymbol{\nu} = [u, v, \omega, p, q, r]^T$ is the (6×1) vector of vehicle linear and angular velocities expressed in the body-fixed reference frame, $\boldsymbol{q}$ is the $(n \times 1)$ vector of joint variables, n is the number of joints, $\boldsymbol{\eta} = [x, y, z, \theta, \phi, \psi]^T$ is the (6×1) vector of vehicle position

and Euler angles in a earth-fixed reference frame, $\boldsymbol{M}(\boldsymbol{q})$ is the $\big((6+n)\times(6+n)\big)$ inertia matrix of the UVMS, $\boldsymbol{C}(\boldsymbol{q},\boldsymbol{\zeta})$ is the matrix of Coriolis and centripetal generalized forces, $\boldsymbol{D}(\boldsymbol{q},\boldsymbol{\zeta})$ is the matrix of friction and hydrodynamic damping terms, $\boldsymbol{g}(\boldsymbol{q},\boldsymbol{\eta})$ is the vector of restoring forces, $\boldsymbol{\tau}=[\boldsymbol{\tau}_r^T,\boldsymbol{\tau}_m^T]^T$, where $\boldsymbol{\tau}_r$ is the (6×1) vector of forces and moments acting on the vehicle and $\boldsymbol{\tau}_m$ is the $(n\times 1)$ vector of generalized joint torques.

Thrusters and control surfaces provide forces and moments on the vehicle according to a nonlinear relation. A simplified relationship can be expressed through the linear mapping [5]

$$\boldsymbol{\tau}_r = \boldsymbol{B}\boldsymbol{u}_r, \tag{2}$$

where $\boldsymbol{B}$ is a $(6\times p)$ matrix, and $\boldsymbol{u}_r$ is the $(p\times 1)$ vector of the p control input; usually, it is $p\geq 6$.

In the case of underwater systems the only significant external disturbance term is due to the ocean current $\boldsymbol{\nu}_c$. A common assumption is to consider the current irrotational and slowly varying; then, the vector expressing the vehicle's velocity in (1) is replaced by the flow velocity vector $\boldsymbol{\nu}_r=\boldsymbol{\nu}-\boldsymbol{\nu}_c$ expressing the relative velocity between the vehicle and the ocean current. By defining $\boldsymbol{\zeta}_r=[\boldsymbol{\nu}_r^T,\dot{\boldsymbol{q}}^T]^T$ the dynamic model (1) can be rewritten in the form [5]

$$\boldsymbol{M}(\boldsymbol{q})\dot{\boldsymbol{\zeta}}+\boldsymbol{C}(\boldsymbol{q},\boldsymbol{\zeta}_r)\boldsymbol{\zeta}_r+\boldsymbol{D}(\boldsymbol{q},\boldsymbol{\zeta}_r)\boldsymbol{\zeta}_r+\boldsymbol{g}(\boldsymbol{q},\boldsymbol{\eta})=\boldsymbol{\tau}. \tag{3}$$

3. Differential Kinematics

For a UVMS the mapping

$$\dot{\boldsymbol{x}}_E=\boldsymbol{J}_E(\boldsymbol{\eta},\boldsymbol{q})\boldsymbol{\zeta} \tag{4}$$

relates the $(6+n)$-dimensional velocity vector $\boldsymbol{\zeta}$ to the m-dimensional end-effector task velocity vector $\dot{\boldsymbol{x}}_E$ through the $\big(m\times(6+n)\big)$ end-effector Jacobian matrix $\boldsymbol{J}_E$. When $(6+n)>m$ the manipulator is kinematically redundant with respect to the given task and $(6+n-m)$ degrees of freedom are available for additional control objectives. Remarkably, this is a common case since the end-effector task is at most expressed in terms of a 6-dimensional position+orientation vector, i.e. $m\leq 6$.

A relevant problem is to invert the mapping (4), because a task for the UVMS is typically specified as a given end-effector motion, while it is of concern to compute the coordinated vehicle+manipulator motion needed to achieve the task. Nevertheless, this problem admits infinite solutions because of system redundancy.

A solution can be written in the form

$$\boldsymbol{\zeta}=\boldsymbol{J}_E^{\dagger}(\boldsymbol{\eta},\boldsymbol{q})\dot{\boldsymbol{x}}_E, \tag{5}$$

where $\boldsymbol{J}_E^{\dagger}$ is the $\big((6+n)\times m\big)$ Moore-Penrose pseudoinverse of $\boldsymbol{J}_E$. This solution has the inconvenience that a given end-effector velocity would in general result in a motion of both the vehicle and the manipulator, which is not desirable from an energy consumption point of view. In addition, the redundant degrees of freedom available in the system are not exploited.

4. Proposed redundancy resolution

To achieve an effective coordinated motion of the vehicle and manipulator while exploiting the redundant degrees of freedom available, we resort to a task-priority redundancy resolution technique [7,8]. In this framework, a primary task $\boldsymbol{\xi}_p$ must be defined which is fulfilled along with a suitably defined secondary task $\boldsymbol{\xi}_s$ as long as the two tasks do not conflict; when the two tasks conflict, the secondary task is released to allow fulfillment of the primary task. The velocity vector $\boldsymbol{\zeta}$ is then computed as [2]

$$\boldsymbol{\zeta}=\boldsymbol{J}_p^{\dagger}\dot{\boldsymbol{\xi}}_p+\Big(\boldsymbol{I}-\boldsymbol{J}_p^{\dagger}\boldsymbol{J}_p\Big)\boldsymbol{J}_s^{\dagger}\dot{\boldsymbol{\xi}}_s, \tag{6}$$

where $\boldsymbol{J}_p$ and $\boldsymbol{J}_s$ are the primary task and secondary task Jacobians, respectively. It can be recognized that the secondary task is given lower priority with respect to the primary task by projecting the relative actions through the null space of the primary-task Jacobian. The obtained $\boldsymbol{\zeta}$ can then be used to compute the position and orientation of the vehicle $\boldsymbol{\eta}$ and the manipulator configuration $\boldsymbol{q}$.

To avoid the typical drift related to numerical integration of the velocity vector, a closed-loop version of solution (6) can be adopted in the form

$$\boldsymbol{\zeta}=\boldsymbol{J}_p^{\dagger}\boldsymbol{w}_p+\Big(\boldsymbol{I}-\boldsymbol{J}_p^{\dagger}\boldsymbol{J}_p\Big)\boldsymbol{J}_s^{\dagger}\boldsymbol{w}_s, \tag{7}$$

where

$$\boldsymbol{w}_p=\dot{\boldsymbol{\xi}}_{p,d}+\boldsymbol{K}_p(\boldsymbol{\xi}_{p,d}-\boldsymbol{\xi}_p) \tag{8}$$

$$\boldsymbol{w}_s=\dot{\boldsymbol{\xi}}_{s,d}+\boldsymbol{K}_s(\boldsymbol{\xi}_{s,d}-\boldsymbol{\xi}_s) \tag{9}$$

in which the subscript d denotes desired values for the relevant variables and $\boldsymbol{K}_p$, $\boldsymbol{K}_s$ are suitable positive definite matrix gains.

As costumary in kinematic control approaches, the output of the above inverse kinematics algorithm provides the reference values to the control law of the vehicle-manipulator system. This control law will be in charge of computing the driving forces aimed at tracking the reference trajectory for the system while counteracting dynamic effects, external disturbances, and modeling errors.

In the case of a UVMS, the primary task vector will usually include the end-effector task vector, while the secondary task vector might include the vehicle position coordinates.

This choice is aimed at achieving station keeping of the vehicle as long as the end-effector task can be fulfilled with the sole manipulator arm. It is worth noticing that this approach is conceptually similar to the macro-micro manipulator approach [4]; the main difference is that the latter requires dynamic compensation of the whole system while the former is based on a kinematic control approach. This would be advantageous for underwater applications in which uncertainty on dynamic parameters may be experienced.

5. Case studies

To demonstrate application of the proposed redundancy resolution technique we have considered a nine-degree-of-freedom UVMS constituted by the Naval Postgraduate School AUV II [6] with a three-degree-of-freedom planar manipulator arm. For the sake of clarity we have restricted our attention to planar tasks described in the plane of the manipulator, that is mounted horizontally. Therefore, we consider six degrees of freedom in the system which is characterized by the three vehicle coordinates x, y, ψ, and the three end-effector coordinates x_e, y_e, ψ_e all expressed in a earth-fixed frame; the three vehicle coordinates z,θ,ϕ are assumed to be constant. A sketch of the system as seen from the bottom is reported in Figure 1, where the earth-fixed, body-fixed, and end-effector reference frames are also shown.

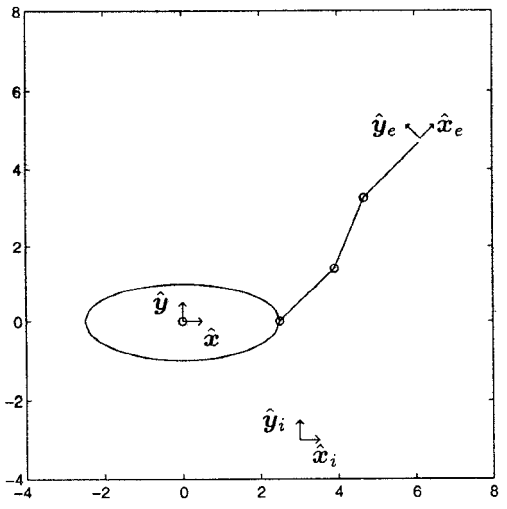

Figure 1 — Underwater Vehicle-Manipulator System.

A station keeping task is considered as first case study. During station keeping, the thrusters must react to the ocean current whose strength exhibits a quadratic dependence on the flow velocity ν_r [5]. However, if we consider the model of the NPS AUV II we can easily recognize that, an ocean current parallel to the $\hat{x}$ axis is not even modelled. This suggests to attempt keeping the fore aft direction of the vehicle aligned with the ocean current in order to reduce energy consumption.

To implement solution (7)–(9), we propose to consider as primary task both the end-effector position+orientation and the vehicle orientation, i.e.

$$\boldsymbol{\xi}_p = \begin{bmatrix} x_e \\ y_e \\ \psi_e \\ \psi \end{bmatrix}, \tag{10}$$

and as secondary task the vehicle position, i.e.

$$\boldsymbol{\xi}_s = \begin{bmatrix} x \\ y \end{bmatrix}. \tag{11}$$

In a first simulation the end-effector has to maintain its position and orientation while the vehicle will change its orientation to minimize the effect of the ocean current; it is desired to keep the vehicle position constant, if possible. Let the initial configuration of the vehicle be

$$\begin{aligned} x &= 0 \\ y &= 0 \quad \text{[m] [rad]} \\ \psi &= 0 \end{aligned}$$

and the manipulator joint angles be

$$\begin{aligned} q_1 &= 1.47 \\ q_2 &= -1.00 \quad \text{[rad]}, \\ q_3 &= 0.30 \end{aligned}$$

corresponding to the end-effector location

$$\begin{aligned} x_e &= 5.92 \\ y_e &= 4.29 \quad \text{[m] [rad]}. \\ \psi_e &= 0.77 \end{aligned}$$

The desired values of the end-effector variables and vehicle position are coincident with their initial value. The desired final value of the vehicle orientation is 0.78 [rad] as given, e.g., by a current sensor; the time history of the desired value ψ_d is computed according to a quintic polynomial interpolating law with null initial and final velocities and accelerations and a duration of 10s. The algorithm's gains are

$$\begin{aligned} \boldsymbol{K}_p &= \text{diag}\{10, 10, 10, 1\} \\ \boldsymbol{K}_s &= \text{diag}\{2, 2\} \end{aligned}$$

The simulation results are reported in Figure 2 and 3.

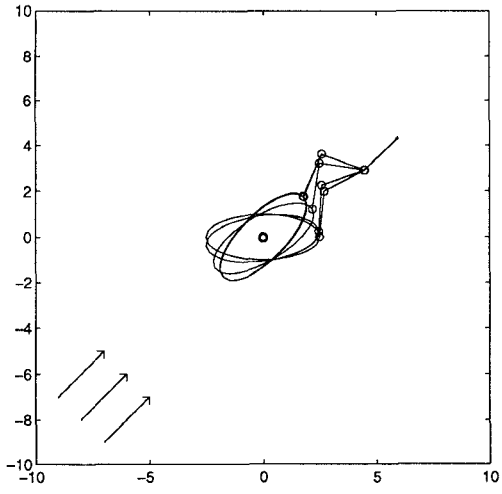

Figure 2 — Re-orientation of the vehicle body with fixed end-effector location.

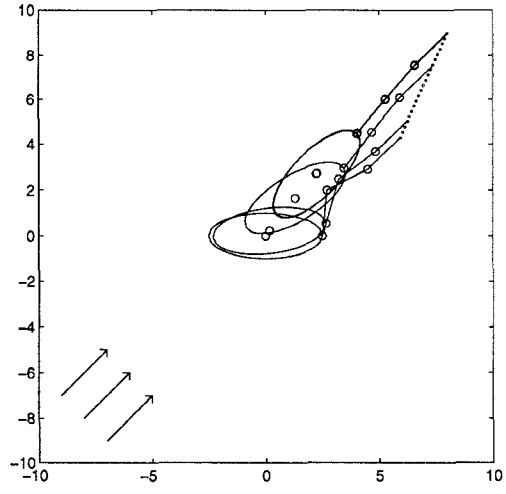

Figure 3 — Re-orientation of the vehicle body with given end-effector trajectory.

It can be recognized that the task is successfully executed, in that the end-effector location and vehicle position are held while the vehicle body is re-oriented to align with the ocean current.

Remarkably, the obtained vehicle reference trajectory is smooth.

A second simulation, starting from the same initial system configuration, considers an end-effector trajectory that cannot be tracked by sole manipulator motion. Therefore, the vehicle must be moved to allow the manipulator end-effector to track its reference trajectory. Also in this simulation, alignment of the vehicle fore aft direction with the ocean current is pursued.

The desired end-effector trajectory is a straight-line motion starting from the same initial location as in the previous simulation and lasting at the final location

$$\begin{aligned} x_e &= 8.00 \\ y_e &= 9.00 \quad \text{[m] [rad].} \\ \psi_e &= 0.78 \end{aligned}$$

The path is followed according to a quintic polynomial interpolating law with null initial and final velocities and accelerations and a duration of 10s. The other task variables and gains are the same as in the previous simulation; remarkably, the desired values of the vehicle position variables are coincident with their initial value also in this case.

The simulation results are reported in Figure 4 and 5.

It can be recognized that the primary task is successfully executed, in that the end-effector location and vehicle orientation achieve their target. On the other hand, the vehicle is moved despite the secondary task demands for station keeping.

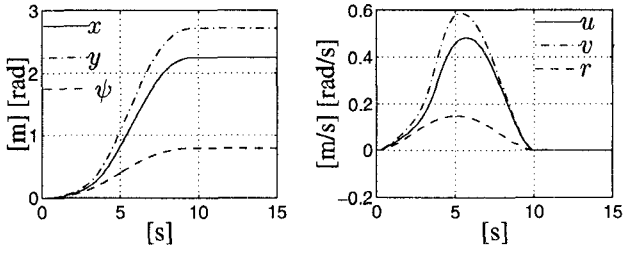

Figure 4 — Time history of vehicle position and velocity variables.

Remarkably, the obtained vehicle reference trajectory is smooth.

To show generality of the proposed approach a second case study has been developed. A drawback of the previous case study might be that the manipulator arm is almost completely stretched out when the end-effector trajectory requires large displacements going far from the vehicle body. Nevertheless, this is related to our choice to keep the position of the vehicle constant and to align the fore aft direction with the ocean current. To overcome this drawback, a different choice of the tasks to be fulfilled is necessary. In particular, we might replace the task of vehicle re-orientation with the task of keeping the manipulator arm in dexterous configurations. To the purpose, it would be possible to use a task variable expressing a manipulability measure of the manipulator arm [11]. In this simple case, it is clear that arm singularities occur when $q_2 = 0$; therefore, the use of q_2 as manipulability task variable would reduce the computational burden of the algorithm.

To implement solution (7)–(9) in this second case study, we thus consider as primary task both the end-effector position+orientation and the second manipulator joint variable,

i.e.

$$\boldsymbol{\xi}_p = \begin{bmatrix} x_e \\ y_e \\ \psi_e \\ q_2 \end{bmatrix}, \tag{12}$$

and as secondary task the vehicle position, i.e.

$$\boldsymbol{\xi}_s = \begin{bmatrix} x \\ y \end{bmatrix}. \tag{13}$$

Starting from the same initial system configuration as before, in the simulation the same end-effector trajectory has been assigned while manipulator joint 2 is driven far from zero; it is desired to keep the vehicle position constant, if possible.

The desired final value of q_2 is -0.78 [rad]; the time history of the desired value $q_{2,d}$ is computed according to a quintic polynomial interpolating law with null initial and final velocities and accelerations and a duration of 10s. The algorithm's gains are

$$\boldsymbol{K}_p = \text{diag}\{10, 10, 10, 1\}$$
$$\boldsymbol{K}_s = \text{diag}\{2, 2\}$$

The simulation results are reported in Figure 6 and 7.

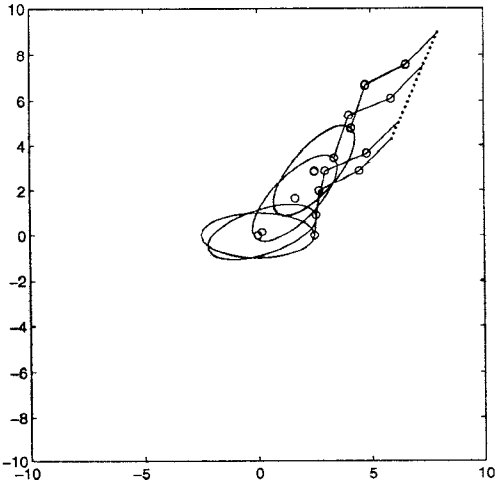

Figure 5 — Tracking of a given end-effector trajectory with manipulator dexterity.

It can be recognized that the primary task is successfully executed, in that the end-effector location and manipulator joint 2 achieve their target. On the other hand, the vehicle is moved despite the secondary task demands for station keeping.

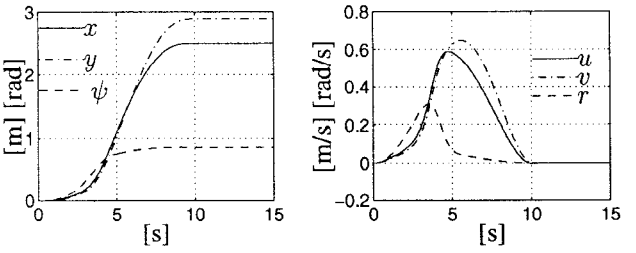

Figure 6 — Time history of vehicle position and velocity variables.

Remarkably, the obtained vehicle reference trajectory is smooth.

To underline the energetic difference in the station keeping task considered in the first case study when executed with and without vehicle re-orientation, a third case study has been developed. Two simulations have been performed considering the full-dimensional dynamic model of the NPS AUV II under a sliding mode control law [1] and the following constant and irrotational current

$$\boldsymbol{\nu}_c = [0.1\sqrt{2} \quad 0.1\sqrt{2} \quad 0\,0\,0\,0]^T.$$

In the first simulation the vehicle stays still and the generalized control forces are required to only compensate the current effect, since the NPS AUV II is neutrally buoyant and $\theta = \phi = 0$. In the second simulation the vehicle moves according to the results of the first simulation in the first case study; thus, the generalized control forces are used to both move the vehicle and to compensate the current effect.

Figure 8 and 9 respectively report the time histories of the 2-norm of the control forces and moments acting on the vehicle as obtained in the two simulations.

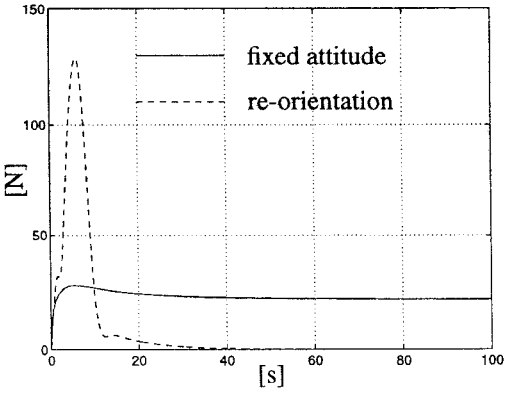

Figure 7 — Time history of the 2-norm of the vehicle forces.

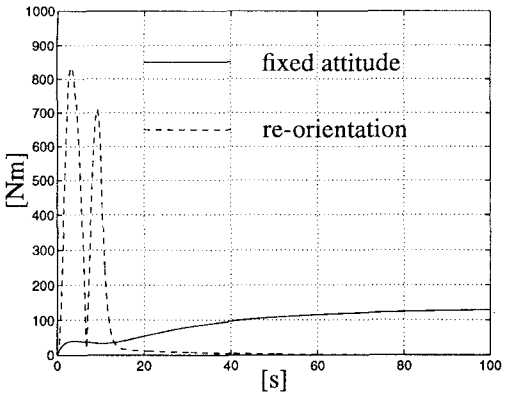

Figure 8 — Time history of the 2-norm of the vehicle moments.

It is easy to recognize that during the reconfiguration the proposed solution is more energy-consuming than the fixed-attitude solution; nevertheless, after the re-orientation has been achieved, the energy consumption required by the proposed technique is negligible. Therefore, the proposed solution becomes the more attractive the longer is the duration of the manipulation task.

For the sake of argument, Table I reports the time integral of the 2-norms of force and moment obtained in the two simulations over a 100s task duration.

	a	b
$\int \|f\|$	2300	800
$\int \|m\|$	9500	5800

Table I — Time integral of the force and moment 2-norms: a) without re-orientation; b) with re-orientation.

6. Conclusions

This paper has addressed the problem of redundancy resolution for underwater vehicle-manipulator systems. A task-priority redundancy resolution approach has been adopted with robustness to the occurrence of algorithmic singularities. Three case studies have been developed to demonstrate effectiveness of the proposed technique in different applications. Simulations have been run on a UVMS constituted by the NPS AUV II carrying a three-link planar manipulator. Redundancy has been exploited first to achieve energy savings and then to increase of system manipulability; a performance comparison has also been developed. Remarkably, the proposed technique is in the framework of kinematic control and thus does not require dynamic compensation actions; this would be advantageous for underwater applications in which uncertainty on dynamic parameters may be experienced.

References

[1] G. Antonelli and S. Chiaverini, "Singularity-Free Regulation of Underwater Vehicle-Manipulator Systems," *Proc. American Control Conference*, Philadelphia, PA, 1998.

[2] S. Chiaverini, "Singularity-Robust Task-Priority Redundancy Resolution for Real-Time Kinematic Control of Robot Manipulators," *IEEE Trans. Robotics and Automation*, **13**(3)398–410, 1997.

[3] S.K. Choi and J. Yuh, "Experimental Study on a Learning Control System with Bound Estimation for Underwater Robots," in *Autonomous Robots*, J. Yuh, T. Ura, G.A. Bekey (Eds.), Kluwer Academic Publishers, pp. 187–194, 1996.

[4] O. Egeland, "Task-Space Tracking with Redundant Manipulators," *IEEE J. Robotics and Automation*, **3**(5)471–475, 1987.

[5] T. Fossen, *Guidance and Control of Ocean Vehicles*, John Wiley & Sons, Chichester, UK, 1994.

[6] A.J. Healey and D. Lienard, "Multivariable Sliding Mode Control for Autonomous Diving and Steering of Unmanned Underwater Vehicles," *IEEE J. Oceanic Engineering*, **18**(3)327–339, 1993.

[7] A.A. Maciejewski and C.A. Klein, "Obstacle Avoidance for Kinematically Redundant Manipulators in Dynamically Varying Environments," *Int. J. Robotics Research*, **4**(3)109–117, 1985.

[8] Y. Nakamura, H. Hanafusa, and T. Yoshikawa, "Task-Priority Based Redundancy Control of Robot Manipulators," *Int. J. Robotics Research*, **6**(2)3–15, 1987.

[9] I. Schjølberg and T. Fossen, "Modelling and Control of Underwater Vehicle-Manipulator Systems," *Proc. 3rd Conference on Marine Craft Maneuvering and Control (MCMC'94)*, Southampton, UK, pp. 45–57, Sept. 1994.

[10] G.E. Schubak and D.S. Scott, "A Techno-Economic Comparison of Power Systems for Autonomous Underwater Vehicles," *IEEE J. Oceanic Engineering*, **20**(1)94–100, 1995.

[11] T. Yoshikawa, "Manipulability of Robotic Mechanisms," *Int. J. Robotics Research*, **4**(1)3–9, 1985.